Journal of Optoelectronics and Advanced Materials Vol. 4, No. 3, September 2002, p. 437 - 454

A SIMULTANEOUS EXPERIMENTAL DETERMINATION OF THE DISTRIBUTION AND CHARACTER OF THE TWO BAND TAILS IN DISORDERED SEMICONDUCTORS

I. Balberg

The Racah Institute of Physics, The Hebrew University, Jerusalem 91904, Israel

While by now the concept of band tails in disordered semiconductors is generally accepted and the evidence for their existence is sound, the experimental determination of their corresponding state distribution and state character are still unsatisfactory. In particular, the quantitative determination of the energy dependence of this distribution for both band tails by the same technique and on the same sample has not been demonstrated. Following these considerations we have developed a phototransport spectroscopy method that consists of two steps. In the first, the photoconductivity, the minority carrier diffusion length, and their light-intensity exponents are measured as a function of temperature. In the second step a comprehensive-systematic simulation study is carried out in order to find the simplest model that yields results that resemble the experimental data. It turns out that our stringent requirement of accounting simultaneously for the behavior of the above four phototransport properties is enough to narrow down significantly the number of plausible scenarios of state distributions in the corresponding pseudogap. The case study we present here, in order to demonstrate our method, is the disordered tissue of single-phase hydrogenated microcrystalline silicon. The achievements, of the application of our method to this system, were culminated in the ability to distinguish between a Gaussian and an exponential band tail, and the determination of the character of the states. In turn, due to the fact that our measurements sense the disordered silicon tissue that encapsulates the crystallites, we are able to demonstrate the generality of the presence of band tails in disordered semiconductors.

(Received June 14, 2002; accepted July 22, 2002)

Keywords: Pseudogap, Band tails, Phototransport

1. Introduction

While it is has been known for a long time that the world around us consists mostly of amorphous systems [1], the problem of their electronic structure, in contrast to that of crystalline solids, was largely "untouchable" [2]. It seems that the reason for that was that the enthusiasm to harvest the consequences of the Bloch theory [3] for crystalline materials lead to the minor attention that was paid to disordered solids. In particular, the long-range order in the crystals (in comparison with the atomic nearest neighbor distances) enabled a straight forward (and applicable) quantum mechanical derivation of their electronic structure [2,3]. Moreover, Bloch's theory established, beyond qualitative arguments, concepts such as electronic bands and sharp band-edges that have been fundamental in the understanding of the optical and electrical properties of crystalline solids. In particular, these concepts are of fundamental importance in the understanding [3] and application [4] of crystalline semiconductors in view of the fact that both the electrical and optical "actions" in these systems take place around the band-edges. Of course, the existence of sharp band-edges follows the strong Bragg-like interference between the propagating and reflected "free-like" electronic waves that create conditions of destructive interference that yield regions of forbidden electronic states [3.5]. There are then sharp band-edges at the top and the bottom of electronic-states bands that consist of a quasi-continuous distribution of allowed states. Correspondingly, it looked also, from the technological points of view, that amorphous solids were unpromising.

Still, in spite of the above well-understood general trend of crystalline solids research, there were attempts to consider possible applications of amorphous covalent solids and to establish some concepts for their understanding. Notably, the works of Kolomiets [6] on the technological end and the works of Mott [7] on the theoretical end have suggested that there might be an interest in amorphous solids in general and amorphous semiconductors in particular. It was then only in the late1960's that the works of Ovshinski [8] have *wide-opened this area of research*, by indicating the potential applications of the latter systems. And, indeed, during the 1970s, the study of amorphous semiconductors became not only of great interest, but was considered then to be the forefront of solid-state physics and technology [9]. The understanding of the latter systems was manifested by the solidification of the concepts developed by Mott [7] and the first [10] attempts to carry out quantitative calculations of the electronic structure of amorphous semiconductors.

As pointed out above, one of the most fundamental concepts in the theory of the electronic structure of crystalline solids, that does not seem to apply to amorphous solids, is that of the sharp band-edges that confine bands of quasi-continuous distribution of states. As the present paper is concerned with the consequences of this conclusion, let us briefly review the concepts that replaced, in a way, the above concept, as attempts were made to describe the electronic structure of amorphous semiconductors [5,9]. Traditionally this description was based on the so-called "chemical approach" [11]. In that picture, that got also a quantitative manifestation [10], the atomic or covalent bond levels split into bands in the solid. Correspondingly, the distribution of the inter-atomic distances or the bond-lengths will cause a distribution of the allowed states around the "band-edge" energy that could be expected in the corresponding (actual or virtual) crystalline counterpart. This picture simply predicts that the overall state distribution will be similar to that found in the "normal" crystalline-material except that the band-edges will be blurred. The degree of the "smearing" around the "normal" band edges appears to depend then on both the inter-atomic distance distribution and the magnitude of the change in the bond-energy due to a given fluctuation around the "normal"-bond length. For example, in the well known model of Cohen Fritzsche and Ovshinsky [12], the relatively large energy shift of some states due to the chemical disorder in amorphous chalcogenides is expected to yield, such a strong "smearing" of the band edges, that there will be a significant energy overlap of states that originate from the bonding (or valence) band and states that originate from the anti-bonding (or conduction) band.

We believe that the "physical picture" that we describe below is somewhat more useful for the qualitative understanding of disordered semiconductors since it yields not only similar consequences regarding the electronic structure, but also a better understanding of the transport properties (as manifested by percolation and tunneling concepts [1,5,9]) in amorphous semiconductors. We start this picture by considering the pre-Bloch free-election model [13]. That model is based on the assumption that the amplitude of the potential undulations in the solid is much smaller than the kinetic energy of the electron. Under these conditions the fact that the potential is not periodic should have little effect on the free-electron-like nature [13] of the allowed quantum states for which no exact destructive interference occurs, i.e. for states that lie "deep" within the bands of allowed states. In fact, since for these states the value of the "crystal momentum" has no consequence as far as destructive interference is concerned, this quantity is essentially as a "good quantum number" in a disordered solid as it is in its crystalline counterpart. The practical meaning of this approach is that we do not expect a significant difference between the electronic properties of a crystalline alkaline-metal and its "amorphous" counterpart, if such would exist. As we consider states of lower kinetic energy we know that under the given potential undulations of the system the interference effects due to the potential undulations will play an increasingly important role yielding, in crystals, an "exact" destructive interference as the band-edge is approached. In the disordered solid the same trend will repeat itself but with the addition that the fluctuations in the (width and height of the) potential undulations will not provide an "exact" destructive interference everywhere in the sample. In other words there will be, a priori, no forbidden states in the system. In covalent materials such as amorphous semiconductors where the packing density of the atoms is roughly the same as in the crystalline counterpart one would expect then that the distribution of the potential undulations would be centered on the corresponding periodic undulations in the crystalline counterpart. As a consequence, some of the states that were close to the band edges in the crystalline counterpart will be higher or lower in their energy than the band-edges. Then, in view of the conservation of the number

of states, there will be, in the disordered semiconductor, a redistribution of (crystalline band) states below and above the band-edges of the corresponding crystalline counterpart.

With further information about the system we can in fact say more about the state distribution. In particular, the strong covalent bonding of the amorphous semiconductors suggests that the probability for a particular deviation in the local structure (e.g. the bond-length and/or bond-angle) will decrease with the magnitude of the corresponding fluctuation. Also, the larger the fluctuation, the larger will be the expected deviation of the energy of a corresponding state from its value in the crystalline counterpart. The last two observations suggest that in amorphous semiconductors, very close to the energy of the (existing or simulated) band-edge of the crystalline counterpart, there will be an inflection point in the state distribution. In particular, due to the conservation of the number of states, the density of states function g(E) will decrease from somewhere above this band-edge towards the mid-band-gap energy of the crystalline counterpart. It appears then that the g(E) concept (unlike the concept of crystal momentum) and its understanding can be carried over from the "physical" theory of crystalline semiconductors to the characterization of the electronic structure in amorphous semiconductors.

In this paper we will be concerned with the experimental determination of g(E) in disordered semiconductors and thus we start by mentioning the relevant concepts that result from the above picture. We define then the *pseudogap* of an amorphous semiconductor as the energy interval for which the crystalline counterpart has its sharp band-edges. Correspondingly, the concepts of the conduction band-edge, E_c, and the valence band-edge E_v, are understood, in the context of the disordered semiconductor, as some "virtual levels", that help us "find our way" in the latter system. In view of the expected distribution of the potential fluctuations we also expect then the decrease of g(E) as the value of E deviates from E_c and E_v, towards the center of the pseudogap. Hence the well-known concept [9,14-19] of *band tail-states* for the corresponding states distribution. Following our understanding of crystalline semiconductors we also expect that the *conduction band tail* (CBT) and the *valence band tail* (VBT) constitute the collection of states that are largely responsible for the electronic and optical properties of disordered semiconductors. To get, however, a somewhat better quantitative feeling for the magnitude of g(E), around and below E_c and E_v, let us recall the following consideration [11]. Since the valence or conduction bands in silicon contain about $2x10^{23}$ cm^{-3} states and the bands are about 5 eV wide, their average destiny of states is about $4x10^{22}$ eV^{-1} cm^{-3}. The many available estimates of g(E) around E_c and E_v in amorphous silicon is that it is of the order of 10^{20} eV^{-1} cm^{-3}. Considering the large drop of g(E) towards the center of the pseudogap we see then that less than a thousandth of the number of band-states has been shifted into the band tails due to the disorder. While a priori this appears as a negligible number, we know that in crystalline semiconductors a much lower concentration of defects affects drastically the electronic properties. In other systems such as the chalcogenides [1,12] this concentration can be larger, and thus, generally, the knowledge of g(E) in the band tails is of crucial importance. On the other hand the low $g(E_c)$ and $g(E_v)$ values enable us to approximate, to first order, the above values of E_c and E_v as the (Mott concept of) mobility edges of the system [1,7,9]. Following our present interest in the electronic structure, rather than in transport, we will ignore here the well-known difference between the two types of edges.

Considering the above mentioned importance of the determination of the electronic structure of disordered semiconductors, for the understanding of their optical and transport properties, the purpose of this paper is to present an experimental spectroscopic method that we have designed not only for the derivation of g(E) but also for the determination of the character of the band tail-states in the pseudogap of a disordered semiconductor. In particular, this method can provide simultaneous information on both band tails and differentiate conclusively between different g(E) dependencies. A particular asset of our method is that it has internal stringent self-consistency requirements that provide very reliable density of states (DOS) maps.

To appreciate the context and the advantages of our method we give in Sec. 2 a brief review of the theoretical expectations of g(E) as well as of the experimental methods that were used thus far for its evaluation. In Sec. 3 we describe briefly the experimental technique and the particular system on which we have chosen to demonstrate our method. Then, in Sec. 4 we describe the essentials of the computational procedure that we use in order to simulate the experimental results. In Sec. 5 we show

the experimental results and in Sec. 6 we review the results of our computer simulations that enable the derivation g(E) map in the entire pseudogap. An overview of this work is given in Sec. 7.

2. Background

2.1 Theoretical expectations

We have argued above that the potential fluctuations (such as the ones that are caused by the stretching of bonds) in a disordered semiconductor are expected to yield a monotonic decrease of g(E) towards the center of the pseudogap. This is in contrast with some defects of very different states, such as the non-bonding states of dangling-bonds, that have energy levels that are a priori removed from E_c and E_v [9]. A simple thermodynamic argument [14] suggests that in the band tails case the DOS distribution g(E) will have an exponential distribution of states that can be defined for the conduction band tail by:

$$N_{ct}(E) = N_{cto}\exp[(E-E_c)/kT_c], \tag{1}$$

Where, $N_{cto} \equiv g(E_c)$, and kT_c is the "width" of the band tail E_{co}. Similarly, for the VBT we have that:

$$N_{vt}(E) = N_{vto}\exp[(E_v-E)/kT_v], \tag{2}$$

where, $N_{vto} \equiv g(E_v)$, and $kT_v \equiv E_{vo}$ is the width of the VBT. In fact it has been suggested [15] that under certain conditions, a Gaussian potential-energy distribution of the disorder induced potential fluctuations can yield such an exponential distribution of states in the band tails. On the other hand, from the many treatments of the problem [9] it appears that such a distribution can lead, depending on the assumption of the relation between the energy of the state, its extent and the number of states, to any distribution between that of a Gaussian band tail, such as [16]:

$$N_{tv}(E) = N_{vto}\exp\{-[E-E_v)^2/2G_{vo}^2]\}, \tag{3}$$

and that of a square-root like band tail, such as [17]:

$$N_{vt}(E) = N_{vto}\exp\{-[E-E_v)/2S_{vo}]^{1/2}\}, \tag{4}$$

Where, G_{vo} and S_{vo} are the corresponding "widths" of the tails. To this date the above are the main distributions under consideration in amorphous semiconductors, although other band tails were also considered [18,19]. Such is, for example, the step-like band tail that can be defined as:

$$N_{vt}(E) = N_{vto} \tag{5}$$

for $E_v \leq E \leq E_v+W_v$, and

$$N_{vt}(E) = 0, \tag{6}$$

for $E > E_v+W$. Numerical computations on large clusters that are feasible these days [20] did reveal indeed strong decreases of the states distributions in the band tails, and these can usually be described as intermediate cases between that of Eq. (3) and that of Eq. (4). A priori, however, the functional dependencies (such as those given in Eqs. (1)-(6)) and the corresponding widths, kT_c, kT_v, G_{co}, G_{vo}, S_{co}, S_{vo}, W_c, and W_v, could not be predicted for a given material and, when computed, they will depend heavily on the assumptions made in the model. As we show below the experimental techniques applied thus far are also quite limited in their ability to yield the correct energy dependence of the state distribution, making the determination of this distribution a well-recognized challenge [21].

2.2 Experimental methods

Turning to the experimental techniques to evaluate states' distributions in amorphous semiconductors in general, and of the band tail states in particular, one faces specific and general problems. Because of space limitations we will mainly emphasize here the latter problems and try to show that our phototransport technique, to be presented in Secs. 3 and 4 overcomes, to a large extent, these general problems.

As a specific example, however, let us consider, the most straightforward methods for the determination of the DOS map in general and in the pseudogap in particular, i.e. optical absorption methods [22]. Ignoring the experimental difficulties in the measurement of weak optical absorption, we note that these methods yield always a deconvoluted DOS map, which depends on assumptions that are made a priori. Moreover, as proposed by Dow and Redfield [23], the "exponential absorption", as implied by the Urbach (disordered induced) absorption is not necessarily due to an exponential band tail [9].

Other types of methods, that were suggested in order to map the DOS distribution over wide energy regions of the pseudogap, are based on purely electrical, or electroptical techniques [9,11]. In the first type of methods, one is usually limited, at best, to one half of the pseudogap due to its dependence on the band bending at the surface. Such are field effect, capacitance-temperature-frequency, and thermally stimulated current, methods. Optoelectronic methods are based on the electrical response to a pulsed (photocapacitance [24] or time of flight spectroscopy [9]) or steady state (photoconductivity) carrier excitations [11]. Of these, the more systematic and comprehensive methods are the Modulated Photocurrent [25] and Transient Photocurrent [26] Spectroscopies. Still, each of the above-mentioned methods has its own difficulties and set of assumptions and, at best, they yield, for a given sample, a DOS map of one half of the pseudogap [22,24-27]. The reason for that is that for all of them, it is *only one, the majority, carrier*, that is being followed by the measurements.

As pointed out above the aim of this paper is to describe a spectroscopic method and its achievements in the determination of detailed and quantitative information on the state distribution in a disordered semiconductor. However, before doing so, let us contrast our approach with that of the many methods that were applied to the most thoroughly studied disordered semiconductor, i.e. hydrogenated amorphous silicon, a-Si:H [9,27,28]. Basically, the common recipe for the derivation of the DOS consists of two stages. First, a theory is developed for the particular interaction of the illumination and/or charge carriers with the pseudogap states, and then, a fit is made of these results to the experimental data by choosing appropriate parameters for the DOS map. The fundamental problem of all the above-mentioned methods is that there are too many parameters involved in the description of the DOS distribution and the character of the states, and thus the experimental data can be fitted by quite a large number of model-scenarios [9,28]. We also note in passing that using a single method does not allow a critical examination of the assumptions made in the model and/or the method of deconvolution [29]. This problem of non-unique deconvolusion has already been realized quite a while ago [9,28] but to this date the deconvolution of a single set of spectroscopic data, according to a pre-chosen model, is the common practice for the derivation of DOS maps [30]. This basic drawback can be solved, at least partially, by trying to fit the same DOS maps to results that come by applying a few spectroscopic measurements to the same sample. Up to now, however, the very few attempts to compare data derived from a couple of different techniques have yielded a further demonstration of the problem rather than its solution [29].

In view of the above we have developed a steady state phototransport method that is based on the simultaneous measurements and analyses of four phototransport properties as a function of temperature. The experimental results of all four dependencies are *required to be fitted by a single* set of DOS map parameters. Indeed, as will be shown in Sec. 6, this is a very stringent requirement but this is what makes the derived DOS map *more reliable and unique* than maps derived by each of the above-mentioned methods. The system that we have chosen for the demonstration of our method is the disordered silicon tissue that encapsulates the crystallites in single-phase hydrogenated microcrystalline silicon, μc-Si:H.

3. A brief description of the present experimental method

Our experimental method is based on phototransport measurements. The determination of the two carriers mobility-lifetime products $(\mu\tau)_e$ and $(\mu\tau)_h$, and their light intensity exponents γ_e and γ_h, as a function of temperature, is carried out in our works [31,32] by the measurements of the temperature, the light intensity, the photoconductivity σ_{ph} and the ambipolar diffusion length L. The above four properties, at each temperature, are derived by applying the relations: $(\mu\tau)_e = \sigma_{ph}/qG$, $(\mu\tau)_h = qL^2/2kT$, $\sigma_{ph} \propto G^{(\gamma_e)}$ and $L \propto G^{(\gamma_h-1)/2}$. Here, q is the electronic charge, G is the photogeneration rate of the carriers and kT is the thermal energy. We note in passing that γ_e and γ_h are differentially sensitive to the DOS distribution [28,33,34]. Our application of these ideas and the adoption of the measurements procedures to a-Si:H and μc-Si:H, using the temperature as the controllable experimental parameter have been described in detail previously [31,32,35] and will not be repeated here. We only mention here that our transport studies were carried out using our standard two (silver evaporated) probe measurements [36] and that in our phototransport measurements we have applied a He-Ne laser illumination that yielded a maximum generation rate of 10^{21} $cm^{-3}sec^{-1}$ carrier pairs.

In the present work we have studied the well-understood system of a-Si:H and the hardly understood system of μc-Si:H. The first system was chosen in order to illustrate the already well-known features of the phototransport in a disordered semiconductor [37], while the phototransport of the other system has not been studied in detail before. For the latter system in its single-phase case, it was shown that 40% of the optical absorption takes place in the disordered tissue that encapsulates the crystallites [38]. This result, and the fact that there is much evidence that polycrystalline silicon, that contains a similar grain-boundary tissue, is electronically composed of two band tails [39-44], suggest that (as explained in detail elsewhere [45]) our measured phototransport properties can be attributed to this tissue. Hence, single-phase μc-Si:H appears to be a good new case for the demonstration of our method in a disordered semiconductor.

The particular a-Si:H system that we studied was prepared by RF glow discharge decomposition of silane [31] and the μc-Si:H samples that we studied were prepared by hot wire (HW) decomposition of silane under very high hydrogen dilution [46]. The substrate used in our study of the transport and phototransport properties was Corning 7059 glass. The preparation of our a-Si:H and μc-Si:H samples and some of their room temperature structural, optical and electrical properties have already been reported [31, 46]. In particular, the typical crystallite size in our μc-Si:H samples is between 10 and 20 nm. For the present purpose, this and the fact that the Raman spectrum analysis has revealed *no a-Si:H phase in the μc-Si:H materials and vice versa* are of great significance since they indicate that each of the systems used in our study constitutes a single phase.

4. A brief description of the computation procedure

On the modeling end, the continuity and charge neutrality equations are solved for a pre-suggested DOS map that is based on some prior knowledge and/or physical expectations of the system under study [47]. In particular, for a-Si:H and μc-Si:H, we followed [31,32,45] quite closely the modeling procedure described in detail by Tran [37]. This enabled us to obtain the model-computed temperature dependencies of $(\mu\tau)_e$, $(\mu\tau)_h$, γ_e and γ_h, as well as the recombination kinetics. For the sake of brevity we will not list here the details of Tran's procedure and the parameters used in our simulations, unless needed for emphasizing a certain point. The ensemble of parameters and the motivation for the particular choice of their values are described in detail elsewhere [45].

In our procedure we have tried various, reasonable, parameters for a given model until the selected parameters yielded a good enough fit to the measured temperature dependencies *of all four properties simultaneously*. Our basic approach is to pre-choose *the simplest model* and try to fit it to the four experimental dependencies. Only after we find, by numerous simulations, with a systematic variation of *all* plausible parameters, that we cannot have a reasonable fit to all four experimental dependencies we move to the next model by adding new types of states to the DOS model. The end result is that we get the *simplest* possible DOS map that accounts for all four sets of experimental

data. Correspondingly, this *stringent self-consistency test* limits the number of DOS scenarios of the maps, and/or their parameter-space, considerably [45, 47].

5. Experimental results

As pointed out above the DOS of a-Si:H is quite well understood by now [31-35,37] and thus we will emphasize here only the qualitative features of the data and give its well-established interpretation without repeating the simulation results that we reported previously [31,32]. On the other hand, we review our results on μc-Si:H in some detail, as for that system no comprehensive DOS map has been reported thus far. We start then with Fig. 1 in which we show the behaviors that we obtained for the temperature dependence of the four phototransport properties in intrinsic a-Si:H. The behaviors shown in Figs. 1(a) and 1(b) have been explained by many researchers as follows [37]. At high temperatures (above, say, 250°K) the carrier recombination is dominated by the dangling bonds. As the temperature is lowered and the quasi-Fermi levels move towards the corresponding band tails the recombination shifts primarily to the donor-like states of the VBT. This causes the sensitization [28,31,32,37] of the electrons' $(\mu\tau)_e$ as manifested by the thermal quenching phenomenon in Fig. 1(a), and the larger-than-unity peak value of γ_e in Fig. 1(b). Our findings [31,32] of the monotonic behaviors of $(\mu\tau)_h$ and γ_h, that are shown in Figs. 1 (c) and 1(d) are, in principle, consistent with this explanation [32]. Below 100°K (not shown here) the recombination is dominated by the CBT states [37].

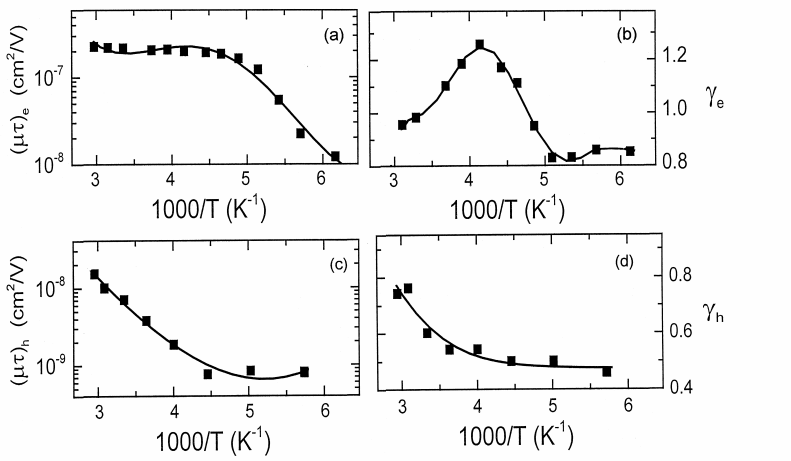

Fig. 1. The typical measured behavior of the temperature dependence of the four phototransport properties in intrinsic a - Si:H films. These results were obtained on samples that were deposited by the glow discharge decomposition of silane (for details see Ref. 31).

Turning to μc-Si:H let us first mention that from the temperature dependence of the dark conductivity of our μc-Si:H samples and from the fact that undoped μc-Si:H is an n-type semiconductor [48,49] we found (by applying the common corresponding procedure [32,36,50] for the determination of the position of the dark Fermi-level, E_F) that E_c-E_F = 0.455 eV.

Having this key parameter we describe now the results of the phototransport measurements that we obtained for our single-phase μc-Si:H. We will avoid here the recombination aspects of the behavior [45] and concentrate on the DOS aspects of the data. Since all the evidence in the literature [48,49] is that undoped μc-Si:H is also an n-type photoconductor, we assumed that the $\mu\tau$ product we derived from the measurement of the photoconductivity, i.e. the $\mu\tau$ product of the majority carriers is that of the electrons. Correspondingly, we denote that $\mu\tau$ product as $(\mu\tau)_e$. In Fig. 2(a) we show then that $(\mu\tau)_e$ increases with temperature. This is well understood to be simply due to the fact that as the

temperature increases the system approaches the "trapping" scenario, i.e., the width of the band gap region (defined by the "demarcation levels" [28,33]) that participates in the recombination is reduced (see Sec. 6). In contrast, the increase of G "takes the system" in the opposite direction, i.e., towards the steady-state "recombination" scenario [28,33,34]. In systems where there is an appreciable concentration of dangling bonds, such as we saw above for a-Si:H, there is a competition between the recombination in the dangling bonds and in the band tail states, so that at the corresponding values of T and G there is a transition (manifested by the non-monotonic features of Figs. 1(a) and 1(b)) from one dominant recombination channel to another. Such a behavior (as we see in Figs. 2(a), and 2(b)) is not repeated here.

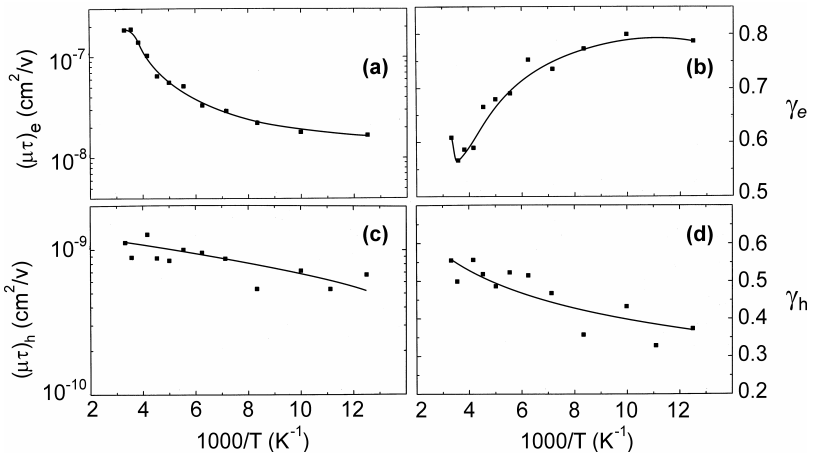

Fig. 2. Our experimentally determined temperature dependence of the four phototransport properties of a sample of single - phase hydrogenated microcrystalline silicon that was deposited by the hot wire technique.

On the other hand in Fig. 2(b) we see a monotonic decrease of γ_e with temperature. This result is consistent with the recombination associated with an exponential distribution of band tail states [33.51]. The corresponding quantitative simplest prediction of the theory of Rose [33], for such a distribution, is that the value of γ_e is given by:

$$\gamma_e = T_c/(T + T_c), \tag{7}$$

where, kT is the thermal energy and kT_c is the width of the exponential CBT. The results shown in Fig. 2(b) are well fitted by a value of kT_c = 28 meV. We should note that in the case of the existence of the two band tails, if the recombination takes place mainly in the VBT, the charge neutrality condition (that forces the shift of the demarcation level [28,33] in the CBT) yields that the value of γ_e will be determined mainly by the width of the CBT [33,51]. The value we found is then in excellent agreement with the well-known CBT width in a-Si:H [22,37] and with the few data [45] on μc-Si:H. The increase of γ_e at higher temperatures is associated with the effect of the band-to-band thermally generated carriers, which will not be discussed here. It is important to note that the temperature dependence of γ_e, in the above [33] and in more complicated cases [28], is determined primarily by the widths of the band tails and only weakly by the capture coefficients of the band-tail states [51].

Following the above conclusion and our rather easy to interpret results, we note that the nature of the states through which the recombination actually takes place is not disclosed by the above-described results. Rather, such results reveal essentially only the nature of the states that enable the charge neutrality compensation [51]. To find the states that are actually associated with the main recombination channel we must follow then the recombination in the states through which this process does take place. In other words, if we adopt the above conclusion regarding the CBT, the above results are *myopic* to the states in which the recombination actually takes place. The latter states, which are then of great interest, can however be revealed by the study of the phototransport properties of the minority carriers, in our case, the holes.

The complementary measurement we were using was designed then for the determination of the phototransport properties of the holes. In Fig. 1(c) we show the results of our measurement of $(\mu\tau)_h$ as a function of temperature. The monotonic increase of this mobility-lifetime product of the minority carriers with temperature is not surprising since it results from the same reason that yielded the monotonic increase of $(\mu\tau)_e$. Indeed, the simultaneous monotonic increases of $(\mu\tau)_e$ and $(\mu\tau)_h$ with temperature are typical, as well as expected [51], in the presence of two band tails. The decisive information here is derived (see Sec. 6), however, mainly from the temperature dependence of γ_h, which is presented in Fig. 1(d). In this figure we see that γ_h is monotonically increasing with temperature but that it has a sub ½ value of γ_h. Such low γ_h, values *cannot be* accounted for, however, by, a single level [33,34,52], a distribution of states that can be approximated by a single effective level [28], or a single exponential band tail [51]. For the cases of two exponential band-tails such values are possible but it can be shown analytically [51], that γ_h will decrease rather than increase (as in our results) with temperature. This can be appreciated, in the simplest case by the expectation that an exponential VBT should yield a $\gamma_h = T_v/(T+T_v)$ type dependence (as expected from Eq. (7) for γ_e). Our experimental results are quite surprising then if one expects that μc-Si:H has two exponential band tails. In order to examine this quite unexpected conclusion, and more importantly, in order to deduce the DOS map in our single-phase μc-Si:H samples, we turned to a comprehensive study of model simulations.

6. Results of the model simulations

As was pointed out above we demonstrate our derivation of the DOS map by considering the data shown in Fig. 2. We started our simulations with the simplest plausible DOS maps finding that we could not reproduce the latter by assuming a single [34] or a two-discrete levels models [52]. Due to space limitations we will not review these attempts here. Rather, we will show the important example that did not yield the above-mentioned agreement and the one that finally yielded such an agreement. We will mention in passing, however, more of the former cases in order to show how our method narrows, in a very significant manner, the number of possible DOS map scenarios. The need to assume a system more complex than that of the single-level centers, the expectation of a continuous distribution of states in the disordered tissue of μc-Si:H and the perfect agreement of the $\gamma_e(T)$ behavior with the simple theory of Rose [33], leave little doubt that there is at least one energy region with a continuous distribution of states in the pseudogap of our material [45]. According to Eq. (7), the behavior we observe for $\gamma_e(T)$ in Fig. 2(b) appears to represent an exponential CBT [33,51] with a width of $E_{co} = 0.03$ eV. Still, since the temperature dependence of γ_e is in principle determined [51] by the combination of both the energy dependence of the DOS in the CBT ($N_{ct}(E)$) and in the VBT ($N_{vt}(E)$) we have checked the above conclusion thoroughly by trying to assume various types of state distributions for either band tail. This included discrete levels, as well as Gaussian, step-like and exponential "square root-like" band tails (see definitions in Sec. 2(a)) for the CBT. In all these cases the results, in particular the $\gamma_e(T)$ and $\gamma_h(T)$ dependencies were very different from the monotonic behaviors shown in Fig. 2. Consequently, and in accord with the existing analytical theories [33,51] and with our simulations with an exponential CBT, we view the $\gamma_e(T)$ dependence as well accounted for by an exponential CBT. We consider the latter to be then a salient feature of our DOS map. Following that conclusion and some available independent evidence [53] we describe here only the results that reproduced the behavior of $\gamma_e(T)$, with an exponential CBT with a width of $E_{co} = 0.03$ eV. Correspondingly, what we tried to resolve then, in particular, is the DOS distribution in the energy region that is not adjacent to the conduction band. Also, as pointed out in Sec. 5, it appears that the concentration of dangling bonds is negligible in comparison with that of other states. Hence, we assume initially that there are no dangling bonds in the system, showing later that this initial assumption is well justified.

Before we consider other plausible states in the pseudogap (as the DOS distribution of the CBT alone can not account for the results) let us remark on the possible character of the centers in the CBT. We found that *very generally* $\gamma_e(T)$ is not sensitive to the corresponding type of centers (neutral-like, donor-like or acceptor-like) but, in contrast, the behavior of $\gamma_h(T)$ is very sensitive to this type. We found then that it was *only* the case of donor-like states in the CBT that yielded (for all the states

distributions that we have tried for the rest of the pseudogap) results that resemble the experimentally observed $\gamma_h(T)$ dependence. Hence, the other salient feature that we concluded from the comparison of the experimental data and the simulation results was that the CBT consists of donor-like states. Correspondingly, *we show below only* results for models that include the above two salient features.

We start our presentation with results of our simulations for a typical case that yields a clear disagreement with the experimental behavior shown in Fig. 2. The case that we have chosen to show is that of the most expected DOS map [37], i.e. that of acceptor-like centers, the states of which belong to an exponential VBT. Let us point out in passing that we have studied this problem thoroughly since it is of importance beyond our present interest in the DOS distribution of μc-Si:H. In particular one expects such band tails in disordered semiconductors in general [9,12,14,15,54] and in amorphous chalcogenides [1,55] in particular.

In Fig. 3 we show then, as an example, the four computed phototransport properties as a function of temperature, for a model that contains an exponential CBT, with donor-like states and a width, E_{co}, of 0.03 eV, as well as an exponential VBT of acceptor-like states. We show this model for the three VBT widths that are illustrated by the right column of the figure. The corresponding DOS maps were derived by considering all the states that participate in the recombination at our $G = 5x10^{19}$ cm^{-3} sec^{-1} generation rate and at 15°K. The latter conditions yield that the map includes practically all the states in the pseudogap. We found that for the reasonable range of exponential VBT widths (i.e. in the range of 10^{-3} to 10^{-1} eV), E_{vo}, the results are in conspicuous disagreement with the experimental results of Fig. 2. While the meaning of the results shown in Fig. 3 will be discussed elsewhere [45], we note already here that while for a relatively wide VBT ($E_{vo} \geq 0.05$ eV) the majority carriers are the electrons, for narrower values of E_{vo} the majority carriers (see below) are the holes. We should point out however that with the possible reasonable range of the μ_e/μ_h ratio in the material, this does not seem to be too significant when we consider the plausible DOS maps [45]. In principle then, the results for all the scenarios shown in Fig. 3 can be interpreted as associated with the electrons as the majority carrier (as is known [48,49] to be the case in undoped μc-Si:H).

Changing the capture coefficients (within the reasonable limits of 10^{-6} to 10^{-15} cm^3sec^{-1}) or the generation rate (within our experimental range) in the simulations have been found to affect some features of the results shown in Fig. 3 but not in a manner that did enhance significantly the resemblance between the computed behaviors and the experimental dependencies shown in Fig. 2. Also, reversing the nature of the types of states in the two band tails yielded results that are even further off the experimental behavior than the results shown in Fig. 3. Following the observation that the VBT is not exponential-like, and before trying other VBT distributions we tried to use a discrete effective level instead of a VBT. The results were found to be not too far off the behavior shown in Fig. 2, but they were not as good as the results to be shown below for the Gaussian VBT. Also, the parameters involved in this model indicated that it represents an effective center rather than a genuine scenario of the state distribution. This scenario is discussed in detail elsewhere [45].

Turning to other possible VBT scenarios we know that, depending on the nature of the disorder that prevails in the semiconductor, various types of band tails, other than exponential, are plausible [18,19,21,56-61]. Following our conclusions from Fig. 3, we turned to check if the results shown in Fig. 2 could be reproduced by any of these non-exponential VBT's. Our systematic study of two square-root-like tails, two step-like-tails or combinations of an exponential with a square-root tail or with a step-like tail (see Sec. 2(a) for definitions) have been found (with any reasonable set of parameters) not to reproduce the behavior shown in Fig. 2. On the other hand, we were able to find a very strong resemblance between our simulation results, for two band tails, and the experimental behaviors shown in Fig. 2, when we assumed a model that included our "standard" exponential CBT and a Gaussian VBT. Correspondingly, we show here only the results obtained with the latter DOS map. Before we describe the above-mentioned results, let us mention that in all our models we have used as a parameter the well known [62] silicon's effective density of states of $N_{vto} = 10^{21}$ $cm^{-3}eV^{-1}$ at E_v (which is well accepted also for disordered silicon systems [37]). The parameter we need here (of which we have no prior knowledge for the present Gaussian band tail case) is the width of the Gaussian VBT, G_{vo}. To find this parameter we searched the whole range of $10^{-1} \geq G_{vo} \geq 10^{-3}$ eV. For a better quantitative agreement with the experimental $\mu\tau$ values we have chosen here a μ_e/μ_h ratio of 10^4 rather than 10 or 100, which is the typical [37] ratio chosen for a-Si:H. The possible reason for this particularly high ratio are discussed elsewhere [45].

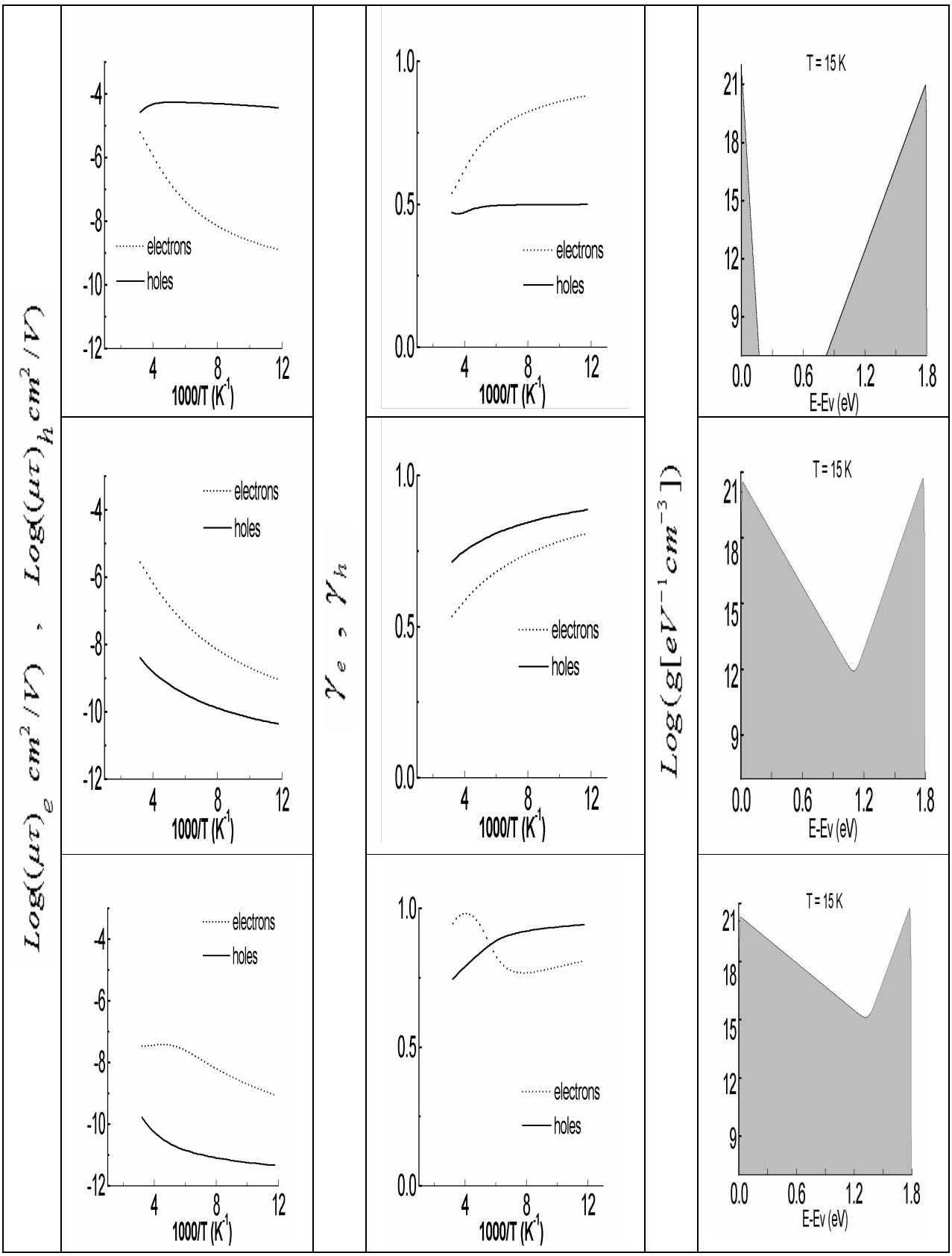

Fig. 3. The simulated temperature dependence of the four phototransport properties, for three widths (0.005, 0.05 and 0.1eV) of the exponential band tail of the valence band. Note that the third column represents the given model of the DOS map in the pseudogap.

The results of our attempts to estimate then the value of G_{vo} are demonstrated in Fig. 4, where we show the temperature dependence of the phototransport properties for three Gaussian VBT widths. These results were derived for the same exponential distribution and parameters that were assumed for the CBT in the simulations that led to Fig. 3. As we see in Fig. 4, for $G_{vo} = 10^{-2}$ eV (the first row) the main discrepancy with Fig. 2 is the temperature dependence of the $\mu\tau$ products. This is improved as G_{vo} increases (in the second row of Fig. 4) to $G_{vo} = 3 \times 10^{-2}$ eV.

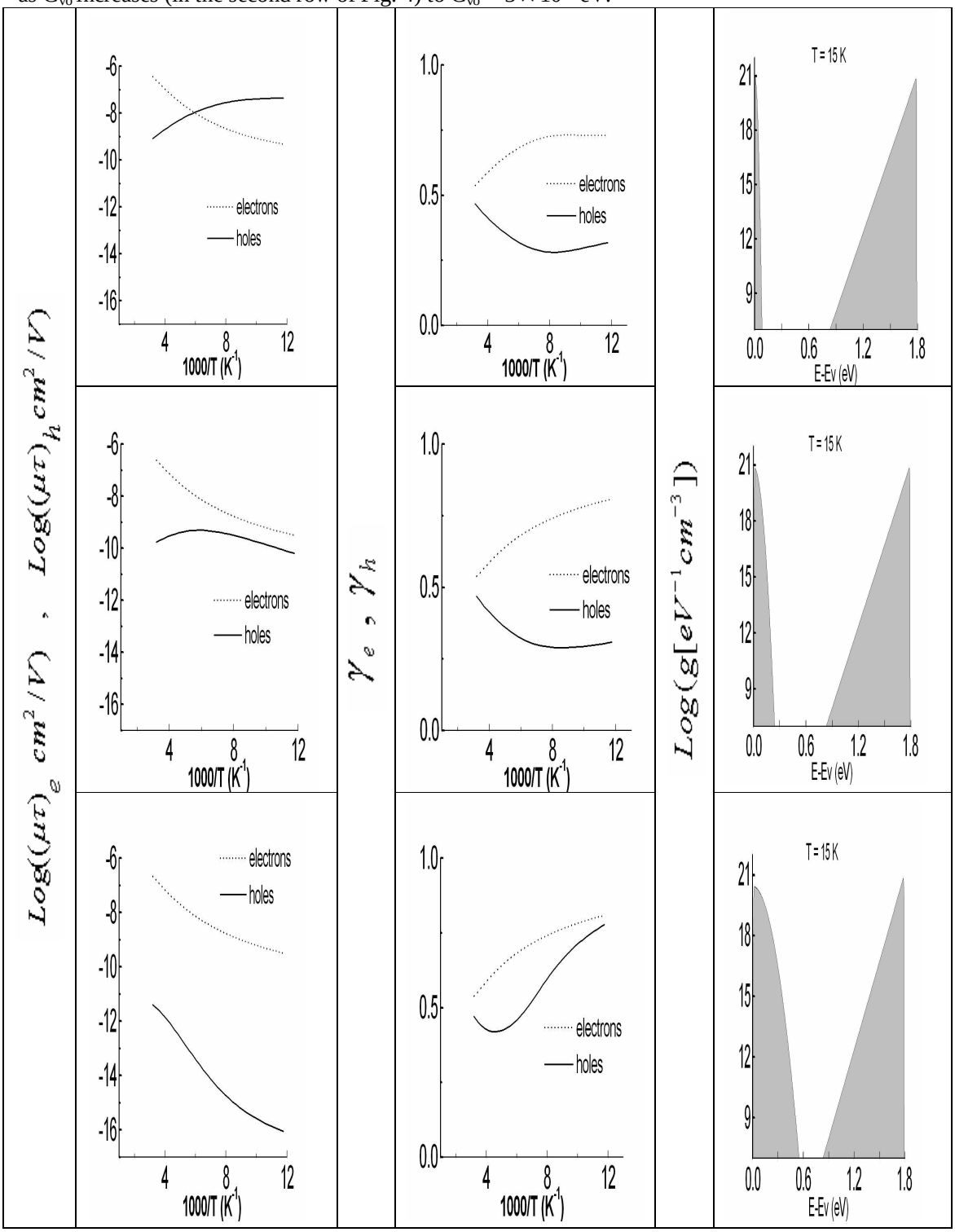

Fig. 4. The simulated temperature dependence of the four phototransport properties for three widths (0.01, 0.03 and 0.07 eV) of a Gaussian valence band tail.

In fact we found that we can reproduce quite well the temperature dependencies shown in Fig. 2 in the relatively narrow interval of G_{vo} values ($10^{-2} \geq G_{vo} \geq 5 \times 10^{-2}$ eV) and that the $G_{vo} = 3 \times 10^{-2}$ eV case is the one that yields the best fit. For higher values, such as $G_{vo} = 7 \times 10^{-2}$ eV (the third row) there is a discrepancy in the behavior of the γ's. As discussed in detail elsewhere [45] one can further improve the quantitative fit of the present model with the experimental data by making reasonable assumptions on the temperature dependence of the system parameters that were used in the derivation of Fig. 4. Here we just mention that, for example, there is a possibility of the narrowing of the band tails with decreasing temperature, which for a-Si:H, has already been shown [63] to account for the weaker experimental behavior in comparison with the one found in the simulations. The important point is however that within a reasonable parameter-space the experimental results can be well reproduced by the scenario exhibited by the DOS map of Fig. 4.

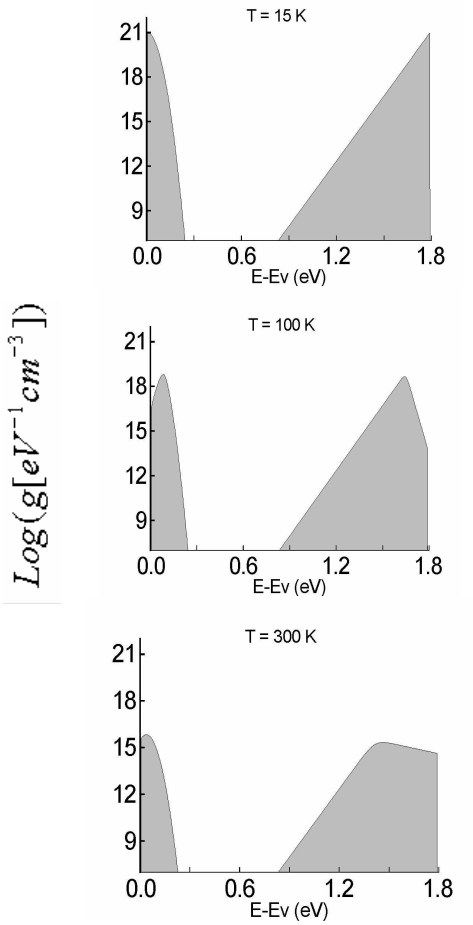

Fig. 5. The DOS maps of the centers that participate in the recombination, at three temperatures. This is for a case that includes a Gaussian valence band tail that yields the behavior exhibited in the second row of Fig. 4.

For completeness we show in Fig. 5 the temperature dependence of the DOS maps of states that participate in the recombination process. These are typical DOS maps for which the results of the second row of Fig. 4 were derived. In passing we note that we can learn here a lot about the recombination process since we see here how the energy range of the states that participate in the recombination, is broadened with decreasing temperature. In fact, the peaks in the band tails are, as far as we know, the first *demonstration that the corresponding Rose concept* [33] of the demarcation level is applicable for a continuous distribution of states, recalling that the demarcation level [33] separates between states the occupation of which is controlled by recombination (the deeper lying states) and the states, the occupation of which, is controlled by "thermal excitation" or "thermal communication" with the band-edges (the shallow states). Here, the peaks separate these two types of

states, and shift to deeper levels as the temperature increases. The position of this peak can be defined then as the demarcation level in the case of a continuous distribution of states. For completeness we have also checked [45] the effect of the addition of dangling bonds to our model. As shown in Fig. 6 we can conclude from the comparison of the simulation results and the experimental data that there are less than $10^{15}cm^{-3}$ dangling bonds in our samples.

Summarizing the results presented in this section, we can conclude that our experimental results suggest that a Gaussian VBT, can account for the experimental data. In contrast, other plausible DOS maps do not seem able to account for that data. We further conclude that the DOS of our single-phase μc-Si:H is very different than that of a-Si:H. On the other hand, as discussed in Sec. 7, the Gaussian VBT scenario is in excellent agreement with many of the DOS maps that were suggested for polycrystalline silicon materials [39-44].

7. Discussion

As we have shown in previous works [31, 32], and above, our requirement of a simultaneous agreement of the temperature dependencies of all four computed phototransport properties with the experimental data is quite a stringent one. In particular this requirement has enabled us to conclude that of the variety of possible model scenarios there is only one that can approximate the actual DOS map in the material under study. In that scenario there is an exponential CBT of donor-like states, with a width of 0.03 eV. We have proven that these characteristics are robust features of the models of the sample under study. As far as we know this is the first experimental proof of how robust and well founded is the Rose [33] prediction for an exponential band tail. Our findings demonstrate the power of the present method for the spectroscopy of the pseudogap states in disordered semiconductors as it enables not only to limit the number of possible DOS scenarios (e.g. the existence and shapes of the band tails) but also to narrow down the parameter space of the DOS scenario that is found (e.g. the determination of the band tail widths) and the character of the states. In particular our method is proven to meet the call [21] (and to overcome the difficulty [64]) to find an experimental method that can determine the shapes of the band tails. This is in clear advantage over the difficulty and complexity of doing that by other methods that were attempted [25,26,64,65] for the same purpose. In particular we were definitely able to distinguish decisively between a Gaussian and an exponential band tail distributions in the DOS map.

The scenario that we found for the DOS map in the vicinity of the valence band was that of a Gaussian VBT that has a width of 0.03 eV. Another new finding in our study is that our experimental results do indicate the absence of dangling bonds. In particular our simulations show that if there are dangling bonds in our samples their concentration is lower than $10^{15}\ cm^{-3}$. While the consequences of this finding on the understanding of μc-Si:H materials are discussed elsewhere [45] we point out here, that in view of our results, we can safely assume that single phase μc-Si:H has, except for the width of its CBT, a very different DOS map than a-Si:H.

Concluding then that a Gaussian-like band tail is the more likely scenario we note in passing that while initially Gaussian band tails were suggested only theoretically [9,16], in recent years such band tails have been proven experimentally, for both organic [56] and inorganic [18,19,66] semiconductors. The finding of a Gaussian band tail is of quite general importance since the transport and phototransport mechanisms in such a band tail may be quite different than in exponential band tails [18,19,66].

Following the above conclusion of a scenario of two band tails but recognizing that our system is different than a-Si:H let us examine our results in comparison with the other system that is expected to be similar to single phase μc-Si:H, i.e. polycrystalline Si. For polycrystalline silicon [39,44,67] it is widely accepted for a long time that there are two band tails, but there is no general agreement on the shape of the band tails. These different conclusions were suggested to be associated with the method of the material preparation [43,44]. In particular, it was pointed out [40] that band tails rather than possible centers of a discrete-level state exist in these systems.

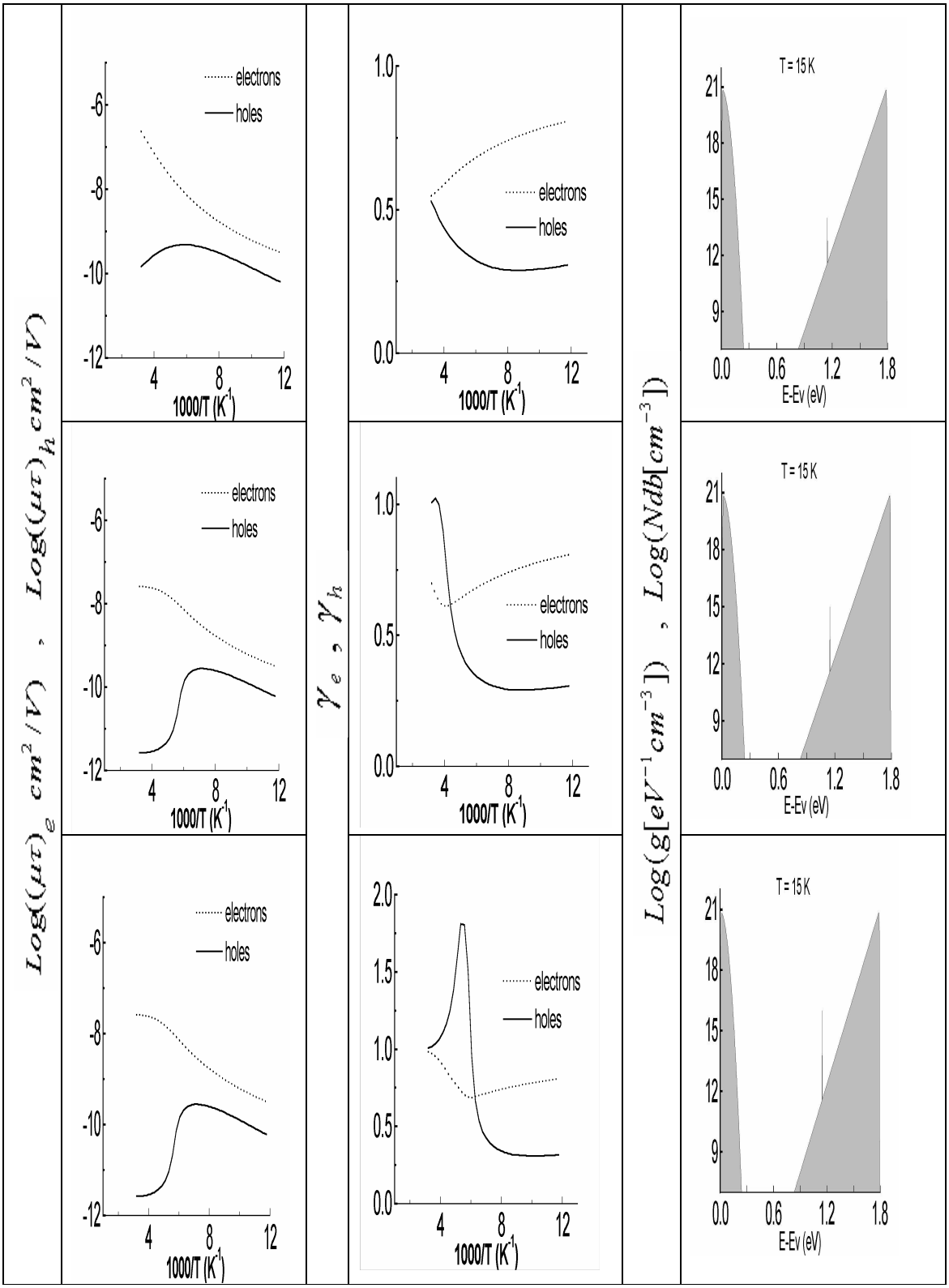

Fig. 6. The effect of the dangling-bond concentration on the behavior of the phototransport properties, for a Gaussian valence band tail (under the conditions that yielded the results shown in Fig. 4 for $G_{vo} = 3 \times 10^{-2}$ eV) for $N_{db} = 10^{14}$, 10^{15} and 10^{16} cm^{-3}.

The most popular model suggested so far for polycrystalline Si materials is that of two double-exponential tails [40-42] (i.e. of two tails such that each of which is made of two different widths in subsequent energy regions of the band gap). Also, a Gaussian CBT tail [44] or a Gaussian VBT [43] has been proposed and the band tail states were attributed to defects in the grain boundaries. We further note that the typical widths of the band tails in polycrystalline silicon are very close to those found here and in a-Si:H [37]. We see then that generally, our conclusion, concerning the state distribution in single-phase μc-Si-H, is more reminiscent of polycrystalline silicon than of a-Si:H. This conclusion does not apply however when we consider the character of the band tail states. For polycrystalline silicon it was usually concluded [40] that the CBT states have an acceptor-like character while the VBT states have a donor-like character. This is not the case for a-Si:H where the character of the band tail states is not well established to this date and different characters of these band tail states have been proposed in different studies [37, 63]. In contrast, in our present comprehensive simulation study we found that only CBT states of a donor-like character can account for the experimental results. On the other hand we found, as in a-Si:H, that the resemblance of the simulation results to the experimental behavior is not sensitive to the character of the VBT states. From the clear disordered-semiconductor character that emerges from our results, it is apparent that the properties we measure are associated with the disordered silicon tissue that wraps the crystallites [45]. We see however that the character of the pseudogap states of this disordered silicon tissue in μc-Si:H is different from that of the corresponding grain-boundary tissue in polycrystalline silicon. The above comparison indicates that while the structural disorder (that affects the DOS map) is similar to that of polycrystalline Si (grain boundaries-like), the formation conditions and the hydrogen atmosphere (that affect the character of the states) are similar to those of a-Si:H.

While the latter conclusions are not too surprising they provide the first experimental evidence that the crystallites encapsulating tissue in μc-Si:H is different from that of the grain boundaries in polycrystalline silicon and that of the homogeneous a-Si:H. This conclusion may be understood by the effects of the Si-H bonds [68-70], in comparison with the former system, and with the "surface character" of the defect (e.g. "bent" bonds [9,71] in the encapsulating tissue) in comparison with the "bulk character" in the latter system. In particular, this suggests that while the states distribution is determined by the structural disorder, it is the hydrogenation [24,68] that may turn around the character of the states. Following the above we conclude then that the Gaussian VBT that we found is the signature of the special phase that we study by phototransport. Further consequences of these findings on the understanding of other properties of μc-Si:H and a-SiH are discussed elsewhere [35,45].

In conclusion, we have presented a self-consistent method for the determination of the DOS map in disordered semiconductors. This method can distinguish between various energy profiles of the band tails as well as the character of the states. In particular, for the disordered tissue of μc-Si:H, we have found these features for the conduction and valence band tails simultaneously, and they are different than those of a-Si:H and polycrystalline silicon.

Acknowledgements

The present work has benefited from the collaboration with A. Catalano, J. P. Conde, V. Chu, Y. Dover, L. F. Fonseca, R. Naidis, Y.Lubianiker, R. Rapaport and G. Wood. This work was supported in part by the Israel Science Foundation and in part by the Enrique Berman solar energy research fund.

References

[1] R. Zallen, The Physics of Amorphous Solids, John Wiley, New York (1983).
[2] N.W. Ashcroft and N.D. Mermin, Solid State Physics, Saunders, Philadelphia (1976).
[3] C. Kittel, Quantum Theory of Solids, John Wiley, New York (1963).
[4] S.M. Sze, Physics of Semiconductor Devices, John Wiley, New York (1969).
[5] J.M. Ziman, Models of Disorder, Cambridge University, Cambridge (1979), Chap. 11.

[6] B. T. Kolomiets, Phys. Stat. Sol. **7**, 359 (1964).
[7] N.F. Mott, Phil. Mag. **31**, 989 (1966) and Adv. in Phys. **16**, 49 (1967).
[8] S. R. Ovshinsky, Phys. Rev. Lett. **21**, 1450 (1968).
[9] For a general review and for many references on spectroscopic methods used for amorphous semiconductors, see: S. R. Elliot, Physics of Amorphous Materials, Longman Scientific & Technical, New York (1990). In particular note the discussion given in pp. 386-389 on the difficulties of obtaining a unique DOS map by some of the common methods.
[10] D. Weaire, M. F. Thorpe, Phys. Rev. B, **4**, 2508 (1971).
[11] For a review see H. Fritzsche, in Physical Properties of Amorphous materials, Eds. D. Adler, B. B. Schwartz, M.C. Steele, Plenum, New York, p. 313, 1985.
[12] M. H. Cohen, H. Fritzsche, S. R. Ovshinski, Phys. Rev. Lett. **22**, 1065 (1969).
[13] J. M. Ziman, Principles of the Theory of Solids, Cambridge University, Cambridge (1965).
[14] Y. Bar Yam, D. Adler, J. D. Joannopoulos, Phys. Rev. Lett. **47**, 467 (1986).
[15] C. M. Soukoulis, M. H. Cohen, E. N. Economou, Phys. Rev. Lett. **53**, 616 (1984).
[16] B. I. Halperin, M. Lax, Phys. Rev. **153**, 802 (1967).
[17] S. Abe, Y. Toyozawa, J. Phys. Soc. Jap. **50**, 2185 (1981).
[18] V. I. Arkhipov, E. V. Emilianova, G. J. Adriaenssens, Phys. Rev. B **64**, 125125 (2001).
[19] S. Grabtchak, M. Cocivera, Phys. Rev. B, **60**, 10997 (1999).
[20] See for example, J. Dong, D. A. Darbold, Phys. Rev. Lett. **80**, 1928 (1998), and references therein.
[21] S. K. O'Leary, P. K. Lim, Solid State Commun. **101**, 513 (1997).
[22] G. D. Cody, in Semiconductors and Semimetals, Ed. J. I. Pankove, Academic, New York, 1986, **21C**, p. 11. For a recent work see for example, K. Rerbal, J.-N. Chazalviel, F. Ozanam and I. Solomon, J. Non - Cryst. Solids **299-302**, 585 (2002).
[23] J. D. Daw, D. Redfield, Phys. Rev. B **5**, 596 (1972).
[24] Y. Lubianiker, J. D. Cohen, H-C. Jin, J. R. Abelson, Phys. Rev. B **60**, 4434 (1999).
[25] For a review see J. P. Kleider, C. Longeaud in Hydrogenated Amorphous Silicon, Pt. 2, Ed. H. Neber-Aeschbacher, Scitec, Zuerich, 1995, p.597.
[26] For a review see, H. Naito in Hydrogenated Amorphous Silicon, Pt. 2, Ed. H. Neber-Aeschbacher, Scitec, Zuerich, 1995, p. 647. For a recent work see, C. Main, J. Non - Cryst. Solids, **299-302**, 525 (2002).
[27] For a review of the most common spectroscopic methods see, Hydrogenated Amorphous Silicon, Ed. Hans Neber-Aeschbacher, Solid State Phenomena, **44-46**, Scitec, Zuerich, 1995.
[28] R. H. Bube, Photoelectronic Properties of Semiconductors, Cambridge University, Cambridge (1992). In particular note the discussion given in pp. 232-233 on the difficulties of obtaining a unique DOS map by only using the temperature dependence of the photoconductivity.
[29] For a consideration of this problem see for example, R. Carius, H. Siebke and J. Folsch, J. Non Cryst. Solids **227-230**, 432 (1998), and S. Reynolds, C Main, D. P. Webb and M. J. Rose, Mater. Res. Soc. Symp. Proc. **557**, 427 (1999).
[30] As an example of the many methods of the single-measurement approach see the temperature dependence of the photoconductivity as described by, G. Schumm, C.-D. Abel and G.H. Bauer, J. Non Cryst. Solids, **137-138**, 351 (1991), and M. Aoucher, T. Mohammed Brahim and B. Fortin, J. Appl. Phys. **79**, 7041 (1996).
[31] Y. Lubianiker, I. Balberg, L. F. Fonseca, Phys. Rev. B **55**, R15997 (1997).
[32] R. Rapaport, Y. Lubianiker, I. Balberg, L. F. Fonseca, Appl. Phys. Lett. **72**, 103 (1998), I. Balberg, R. Naidis, L. F. Fonseca, S. Z. Weisz, J. P. Conde, P. Alpuim, V. Chu, Phys. Rev. B **63**, 113201 (2001), L.F. Fonseca, S.Z. Weisz, R. Rapaport and I. Balberg, Mater. Res. Soc. Symp. Proc. **557**, 439 (1999), and L. Fonseca, S.Z. Weisz and I. Balberg, Mater. Res. Soc. Symp. Proc. **664**, in press.
[33] A. Rose, Concepts in Photoconductivity and Allied Problems, Interscience, New York (1963).
[34] I. Balberg, J. Appl. Phys. **75**, 914 (1994).
[35] I. Balberg, J. of Non - Cryst. Solids **299-302**, 531 (2002).
[36] Y. Lubianiker, I. Balberg, Phys. Rev. Lett. **78**, 2433 (1997) and, M. Rashotko and I. Balberg, Appl. Phys. Lett. **78**, 763 (2001).
[37] For a detailed discussion of experimental results and simulations of the phototransport

properties in a-Si:H-like materials, as well as corresponding references, see M.Q. Tran, Phil. Mag. **B, 72**, 35 (1995).
[38] See for example, F. Diehl, M. Scheib, B. Schroder, H. Oechsner, J. Non - Cryst. Solids **227-230**, 973 (1998).
[39] For a collection of reviews see, Polycrystalline Semiconductors, Ed. G. Harbeke, Springer-Verlag, Berlin (1985). For a comprehensive introduction see W. Monch, Semiconductor Surfaces and Interfaces, Springer, Berlin (1995).
[40] O. K. B. Lui, S. W. B. Tam, P. Migliorato, T. Shimoda, J. Appl. Phys. **89**, 6453 (2001).
[41] J. R. Ayres, J. Appl. Phys., **74**, 1787 (1993) G. A. Armstrong, J. R. Ayres, S. D. Brotherton, Solid State Electronics **41**, 835 (1997).
[42] S. S. Chen, J. B. Kuo, J. Appl. Phys. **79**, 1961 (1996).
[43] T. J. King, M. G. Hack, I. W. Wu, J. Appl. Phys. **75**, 908 (1994).
[44] C. A. Dimitriadis, J. Appl. Phys. **73**, 4086 (1993).
[45] For details, see I. Balberg, Y. Dover, R. Naidis, J. P. Conde, V. Chu, Phys. Rev. B, to be published**.**
[46] P. Alpuim, V. Chu, J. P. Conde, J. Appl. Phys. **86**, 3812 (1999), P. Brogueira, V. Chu, J. P. Conde, Mater. Res. Soc. Symp. Proc., **377**, 57 (1995). and references therein.
[47] Y. Lubianiker, G. Biton, I. Balberg, T. Walter, W. H. Schock, O. Resto, S. Z. Weisz, J. Appl. Phys. **79**, 876 (1996).
[48] R. Bruggemann, C. Main, Phys. Rev. B **57**, R15080 (1998).
[49] M. Goerlitzer, N. Beck, P. Torres, J. Meier, N. Wyrsch, A. Shah, J. Appl. Phys. **80**, 5111 (1996).
[50] H. Overhof, P. Thomas, Electronic Transport in Hydrogenated Amorphous Semiconductors, Springer-Verlag, Berlin (1989).
[51] M. Hack, S. Guha, M. Shur, Phys. Rev. B **30**, 6991 (1984).
[52] Y. Simovitch, Y. Dover, I. Balberg, unpublished.
[53] R. Bruggemann, J. P. Kleider, C. Longeaud, D. Mencaraglia, J. Guillet, J. E. Bour`ee, C. Niikura, J. Non Cryst. Solids, **266-269**, 258 (2000), and T. Unold, R. Buggermann, J. P. Kleider, C. Longeaud, ibid, p. 325, and J.P. Kleider, C. Longeaud, R. Buggermann and F. Houze, Thin Solid Films **383**, 57 (2001).
[54] See for example, E.N. Economou, C. M. Soukoulis, M. H. Cohen, A. D. Zdetsis, Phys. Rev., B **31**, 6172 (1985), see also E. N. Economou, C. M. Soukoulis, M. H. Cohen and S. John, in Disordered Semiconductors, Eds. M. A. Kastner, G. A. Thomas and S. R. Ovshinsky, Plenum, New York, 1987, p. 681.
[55] For a recent collection of reviews see Proc. of the 2nd Int'l Conference on Amorphous and Nanostructured Chalcogenides, published in J. of Optoelectronics and Advanced Materials (2001), in particular see I. Balberg, ibid p. 587.
[56] M. Pope, C. E. Swenberg, Electronic Processes in Organic Crystals and Polymers, Oxford University, Oxford (1999).
[57] A. A. Klochikhin, S. G. Ogloblin, Phys. Rev. B **48**, 3100 (1993).
[58] A. A. Klochikhin, Phys. Rev. B **52**, 10979 (1995).
[59] M. C. W. Van Rossum, Th. M. Nieuwenhuizen, E. Hofstetter, M. Schreiber, Phys. Rev. B **49**, 13377 (1994).
[60] V. I. Arkhipov, G. J. Adriaenssens, Phys. Rev. B **54**, 16696 (1996), and D. V. Nikolaenkov, V. I. Arkhipov and V. R. Nikitenko, Semiconductors **34**, 655 (2000), and references therein.
[61] D. Redfield, Adv. in Phys. **24**, 463 (1975).
[62] R. Smith, Semiconductors, Cambridge University, Cambridge (1961).
[63] F. Wang, R. Schwarz, Phys. Rev. B **52**, 14586 (1995).
[64] S. Grabtchak, C. Main, S. Reynolds, J. Non Cryst. Solids **266**, 362 (2000), and D. P. Webb, C. Main, S. Reynolds, Y. C. Chan, Y. U. Lam, S. K. O'Leary, J. Appl. Phys. **83**, 4782 (1998).
[65] C. Longeaud, J. P. Kleider, Phys. Rev. B **45**, 11672 (1992).
[66] C. E. Neble, R. A. Street, N. M. Johnson, J. Kocka, Phys. Rev. B **46**, 6789 (1992).
[67] A. Heya, A.-Q. He, N. Otsuka, H. Matsumura, J. Non - Cryst. Solids **227-230**, 1016 (1998).
[68] S. B. Zhang, H. M. Branz, Phys. Rev. Lett. **84**, 967 (2000).
[69] R. Krankenhagen, M. Schmidt, S. Gerbner, M. Poschenrieder, W. Henrion, I. Sieber, S. Koynov and R. Schwarz, J. Non Cryst. Solids **198-200**, 923 (1996).
[70] D. Kurnia, R. P. Barclay, J. M. Boud, J. Non - Cryst. Solids **137**, 375 (1991).
[71] H. Shirai, T. Arai, J. Non - Cryst. Solids **198-200**, 931 (1996).